CROATIAN MEDICAL JOURNAL
CMJ

44(4):463-468,2003

CLINICAL SCIENCES

Magnetic Resonance Imaging of Immune Cells in Inflammation of Central Nervous System

Istvan Pirko[1], Bogoljub Ciric[2], Aaron J. Johnson[4], Jeff Gamez[1], Moses Rodriguez[1,2], Slobodan Macura[3]

Departments of Neurology, [2]Immunology, and [3]Biochemistry, Mayo Clinic, Rochester, Minn; and [4]Department of Immunology, University of Washington, Seattle, Wash, USA

Aim. To develop a novel, magnetic resonance-based method for in vivo cell localization in the central nervous system (CNS) of the animals without sacrificing them.

Methods. Cells were labeled in vivo by intravenous injection of cell marker-specific antibodies covalently bound to ultrasmall superparamagnetic iron oxide particles (USPIO). This enabled the visualization of specific cell types by magnetic resonance microscopy (MRM).

Results. USPIOs covalently attached to antibodies affected the contrast in MRM scan, and their accumulation on cells manifested as signal weakening in T2*-weighted images or signal enhancement in T1-weighted images. With this method applied in the experimental autoimmune encephalomyelitis (EAE) murine multiple sclerosis (MS) model, CNS-infiltrating $CD4^+$ T cells were easily visualized with cell-specific MRM.

Conclusion. MRM with targeted contrast materials can be used to localize CNS-infiltrating lymphocytes of interest. Due to its noninvasive character, this method could potentially be used in human MR imaging as well.

Key words: *contrast media; CD4-positive T-lymphocytes; encephalomyelitis, experimental autoimmune; magnetic resonance imaging; models, animal*

To study the pathophysiology of multiple sclerosis, several disease models have been developed. Perhaps the best known and most utilized is experimental autoimmune encephalitis, an autoimmune disease characterized by immune response against different myelin epitopes. In most experimental autoimmune encephalitis models, the primary mediators of the autoimmunity are central nervous system (CNS)-infiltrating $CD4^+$ T cells specific for one or more myelin proteins (1,2).

A common aim in medicine is to visualize immune cells participating in immune-mediated inflammatory diseases. Traditionally, cell visualization is done by immunohistochemical staining, where specific antibodies against immune cells or proteins of interest are introduced to tissue samples. These antibodies are labeled either with fluorescent markers or with enzymes that can catabolize a chromogenic substrate. These methods give accurate, reproducible, and universally accepted results. However, a major drawback is that the studied animals need to be sacrificed. Thus, for a given number of animals, these methods allow only "static" investigations. For dynamic studies, more animals are required, because at each time point a group of animals has to be sacrificed. This results in groups needing to be larger to minimize the effects of biological variability. For these reasons, noninvasive methods are highly desirable. This is particularly important from the prospective of applying cell-imaging methods to human medicine.

Magnetic resonance (MR) is widely used for noninvasive studies of biological systems. When used to generate images of macroscopic objects (usually with millimeter resolution), it is called MR imaging (MRI) (3), and when images reach submillimeter resolution (in smaller objects) it is called MR microscopy (MRM) (4).

Besides being noninvasive, an important advantage of MRI is the availability of numerous physicochemical parameters to modulate the image contrast. For example, MR images can be weighted by spin density (water concentration), relaxation times (T1, T2, T2*, or T1ρ), diffusion coefficient (D), efficacy of magnetization transfer between macromolecules and water (magnetization transfer), chemical shifts, as well as by their various combinations, such as T1/T2, D*T2, and so on. In spin density, MRI detects signal

from water protons. Image is recorded immediately after system perturbation, so all spins contribute the same to the signal intensity and picture brightness depends on the spin concentration. In T1-weighted imaging, before image recording the system is kicked out of equilibrium and brought into new steady state where spins that relax quickly recover more than slowly relaxing spins. Then, the image brightness, in addition to spin density, is weighted by T1 relaxation rates. In T2-weighted imaging, the system is kept initially in equilibrium and the image is recorded some time after perturbation. Spins that have long T2 relaxation times will contribute more to the signal than spins with short T2. For example, gray and white brain matter have different T2 relaxation times and in T2 weighted images are nicely delineated. In T2-weighted images the influence of local magnetic field inhomogeneity is eliminated; the contrast is affected only by the differences on molecular level. In T2* imaging, influence of local magnetic field is preserved. The higher the local field inhomogenity, the less signal is recovered. Thus, in T2*-weighted image, besides molecular properties, microscopic (and macroscopic) field inhomogeneity affects the contrast.

Because some of these parameters depend on the physiological state of the tissue, MR-based methods can be used to monitor physiological parameters in vivo. For example, blood oxygenation levels affect proton T2 relaxation and can be used to monitor brain activity (5). Similarly, the chemical shift of ^{31}P nuclei in inorganic phosphate depend on both pH and temperature, and can be used to determine intracellular pH or local tissue temperature (6,7).

The versatility of MRI is further improved by the introduction of external agents that affect the image contrast (8,9). The two most notable are paramagnetic metal complexes (Gd, Mn, and Fe) and (ultra)small paramagnetic iron oxide particles, or (U)SPIOs. USPIO particles affect the field homogeneity in their immediate surroundings and in T2* images show up as a darkened areas. USPIOs do not affect spin environment on the atomic scale and, thus, do not affect contrast in T2 images. The presence of a contrast agent changes the relaxation of spins in the surrounding tissue, revealing the agent's spatial distribution. For example, gadolinium-diethylenetriaminepentaacetate (Gd-DTPA) enters the brain from the bloodstream only if the blood-brain barrier is compromised. In T1-weighted images, this may reveal the location of tumors, abscesses, or inflammation. Even more potent are "smart" contrast agents that selectively accumulate in specific regions of interest. A region of interest may be an organ/tissue, cell aggregates (tumors or lesions) or specific compounds (enzymes, enzyme substrates, amyloid plaque, or fibrils) (10,11).

Good contrast agents need to fulfill several requirements (9). They should affect one or more image parameters in a predictable way, be delivered to the targeted region, be cleared in a reasonable period of time, and be nontoxic. The unmodified USPIO-based contrast agents already fulfill the first and last requirement: USPIOs are insoluble under physiological conditions and are nontoxic in the doses used for MR (8). Because of their superparamagnetism, USPIO particles considerably deteriorate magnetic field homogeneity in their immediate vicinity. The observed decrease of local field homogeneity results in shortening of local T2* of surrounding nuclear spins, causing the MR signal attenuation in the immediate vicinity of USPIOs. Thus, in T2*-weighted MR images, USPIOs act as a negative contrast agent (8). USPIOs also affect T1 relaxation rates of nearby protons, but this effect is considerably weaker compared to T2. Thus, in T1-weighted MR images, USPIOs act as a positive contrast agent since the regions with faster T1 relaxation look brighter in the images (9).

Central to contrast agent design is the selectivity and reproducibility of the agent's delivery into a targeted region. A suitable carrier provides the specificity of these agents. For example, the delivery of USPIOs in a cell-specific manner requires the attachment of USPIOs to a cell-specific transporter. Various attempts have been made to visualize immune cells by MRI (12-19). Some of the best-known efforts are macrophage-labeling experiments (19). This approach exploits a pronounced feature of macrophage biology to internalize various organic and inorganic materials by phagocytosis. Thus, the labeled particles can be relatively easily "implanted" in these cells. However, to label other immune cells, there is no established and universally accepted method.

Because of high specificity, antibodies represent particularly attractive carriers for smart contrast agent design (12-19). By the use of monoclonal antibodies labeled with USPIOs, our laboratory has successfully implemented an easily reproducible approach for labeling specific immune cells in vivo.

Here we describe the use of commercially available superparamagnetic microbeads as MR contrast materials. Microbeads are routinely used for magnetic cell sorting (MACS), DNA and RNA purification, and immunoassays (20). These microbeads are called SPIOs or USPIOs (depending on the size of the magnetic particle). For cell separation (and our experiments), microbeads are covalently attached to antibodies or Fab fragments. The size and chemical composition of microbeads from different sources vary considerably, which can dramatically influence their applicability in MRI. Microbeads could be as small as 30-50 nm in diameter, which makes them about one million times smaller in volume than eukaryotic cells. Microbeads form a stable colloidal suspension and do not sediment or aggregate in magnetic fields. They typically do not activate cells or influence function and viability of the cells to which they are attached. Furthermore, microbeads are readily biodegradable under normal physiological conditions and nontoxic in quantities used in imaging procedures. We demonstrate this imaging method by visualizing $CD4^+$ immune cells infiltrating the CNS of mice with experimental autoimmune encephalitis.

Material and Methods

Experimental Autoimmune Encephalitis Induction in Mice

The Institutional Animal Care and Use Committee approved all studies. Adoptive experimental autoimmune encephalitis in female SJL/J mice (Jackson Laboratories, Bar Harbor, ME, USA) was induced with myelin basic protein (MBP) peptide Ac89-101 as described elsewhere (2,21). Donor mice were immunized in flanks with 200 μL of the MBP-peptide emulsified in complete Freund's adjuvant (CFA; 200 μg peptide, 200 μg *M. tuberculosis* H37 RA). Draining lymph nodes and spleens were removed 12 days later and a single-cell suspension was prepared. Cells were cultivated for four days in media containing 25 μg/mL of MBP-peptide. After four days, 4×10^7 cells, harvested from the cell-culture, were injected intraperitoneally. The first clinical symptoms of experimental autoimmune encephalitis appeared 7-10 days after cell transfer. Maximum symptoms were seen between day 10 and 20 after transfer.

One day prior to imaging, the mice were injected with 20 μL superparamagnetically labeled antibodies specific for murine CD4 or human CD19 (Miltenyi Biotec, Gladbach, Germany) (22-26).

Magnetic Resonance Imaging (MRI)

MRI was performed at 7 Tesla on a Bruker Avance 300 (wide bore) NMR spectrometer (Bruker Biospin, Billerica, MA, USA) equipped with imaging accessories. The animal body temperature was maintained at 37 °C by a flow of conditioned air. During imaging, the mice were anesthetized by isofluran (1.5% in oxygen) delivered via a nose cone. We recorded 3D images to enable geometric matching of areas of interest from scans obtained on the same animal at different times, and to compare MR images with histological specimens. T1-weighted spin-echo sequences (TR: 200 ms, TE: 6.2 ms) with 3D volume acquisition were used to visualize the labeled antibodies (FOV: 3×2×2 cm; matrix: 160×90×90; acquisition time: 27 minutes). T2*-weighted 3D images (TR: 120 ms, TE: 10 ms, FA: 15, NEX: 4) were recorded with FOV 3×2×2 cm and matrix size 160×90×90 within 61 minutes. Image analysis, reconstruction, and slice selection were done by using the ParaVision software package, supplied with the spectrometer (Bruker Biospin).

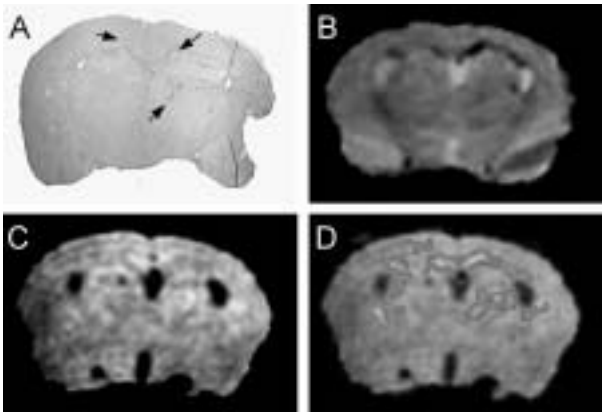

Figure 1. Comparison of histology with cell-specific magnetic resonance imaging (MRI). **A.** Immunohistochemistry of coronal brain section of B6 mouse infected with Theiler's Murine Encephalitis Virus (TMEV) through the hippocampus; CD8 T-cell labeling. Dark dots represent the location of CD8 cells in the parahippocampal areas and in the right thalamus (arrows). **B.** Corresponding T2*-weighted MR image, where areas of negative contrast (low signal) show the location of ultrasmall superparamagnetic iron oxide particles (USPIO)-labeled anti-CD8 antibodies. **C.** On the T1-weighted image, areas of high signal correspond well with the location of CD8 cells on histology (A), and depict the location of USPIO antibodies. **D.** Composite MRI image of the same animal *in vivo*, after administration of USPIO-labeled anti-CD8 antibodies. A mask was generated by dividing the T1-weighted image (C) by the T2*-weighted image (B). Since we observe positive contrast on T1 and negative contrast on T2*-weighted images with the application of USPIO-labeled antibodies, the mask generated by matrix division will contain high numbers ("bright areas") where the corresponding T1 image matrix value was high and T2* image matrix value was low.

Results

We demonstrated the principle of cell-selective MR imaging on an example of CD8 labeling in C57B6/J mice infected with Theiler's Murine Encephalitis Virus (TMEV), which we described in details elsewhere (27). A microscopic image of coronal brain section of a B6 mouse showed the location of $CD8^+$ cells enhanced with immunohistochemical staining (Fig. 1A). On the corresponding T2*-weighted MR image obtained from the same mouse in vivo, the areas of USPIO accumulation presented as dark regions (Fig. 1B). On a T1-weighted image, the same regions were brighter (Fig. 1C). The difficulty of observing negative contrasting in noisy T2* images and weak contrasting of USPIOs in T1-weighted images can be overcome by suitable combination of the two images. One possibility is to create a mask based on the ratio of the two images, which will emphasize only the regions where simultaneously T2*-weighted image yield negative contrast and T1-weighted image yield positive contrast. Figure 1D shows such a mask (generated from the ratio of the two images, T1/T2*) superimposed on the T1 image. With the help of mask regions of USPIO accumulation, the lesions are clearly visible. After identifying the lesions with the help of the mask, repeated inspection of the T1-weighted image can clearly allow identification of faint regions of positive contrast (Fig. 1C). Although reading T1 images is somewhat less obvious than reading T2* images, their main advantage is less time requirement and immediate availability on every system. Also, T2* images are obtained by gradient echo sequences, which are endogenously more prone to artifacts than the spin echo sequences used for T1-weighted image acquisition. We therefore chose to focus on T1-weighted MR images.

In the experimental autoimmune encephalitis experiment, six mice were imaged 14, 21, 25, and 28 days after induction of experimental autoimmune encephalitis. CD4 labeling was done each day prior to imaging. Until day 21, no specific relaxation enhancement was seen on the obtained images. Each panel of T1-weighted images of different brain and spinal cord areas of animals with experimental autoimmune encephalitis shows the same cross-sections with 8-bit and 3-bit representation (Fig. 2). The latter, while devoid of subtle details visible in the standard image, helps the untrained eye to observe regions of increased T1 relaxation rates, ie, accumulation of labeled $CD4^+$ T-cells. The localization of the labeled cells in various areas of the brain is clearly outlined, including the brain stem, cerebellum, parahippocampal, frontal, and prefrontal areas (Fig. 2, panels A-D). Thus, T1-weighted images in either representation (8-bit or 3-bit) are capable of visualizing USPIO-

labeled CD4+ T-cell accumulation in mice with experimental autoimmune encephalitis.

To monitor the time course of experimental autoimmune encephalitis development in SJL mouse brain, we recorded T1 images at regular time intervals. Figure 3 shows four time points: day 14, 21, 25 and 28, with strong enhancement visible on days14-21, less on day 25, and almost none on day 28.

Discussion

USPIOs are known to have strong T2 and T2* effects ("negative contrast material"); yet their T1 effect ("positive contrast material") has not been exploited. The fact that these particles accumulate at sites of interest can explain why they also have T1 effects, thus providing "positive contrast". Positive contrast materials are considered superior to negative contrast materials since it is easier to localize high-signal areas on homogenous, relatively less detailed T1-weighted images compared with localizing a low-signal areas on highly detailed T2- or T2*-weighted images. The same areas that show up as "low signal" on T2*-weighted images a few hours after injecting the targeted contrast material, will later correspond with "high signal" areas on T1-weighted scans (approximately 12-24 h after injection, Fig. 1).

We think that biodegradability of the microbeads we used may actually be an important factor in their capability to serve as contrast material. During the experiments, we noticed that microbeads are detectable at the sites of their accumulation first on T2*-weighted images and only after several hours delay on T1-weighted images. This may indicate that a secondary event beside the accumulation of microbeads took

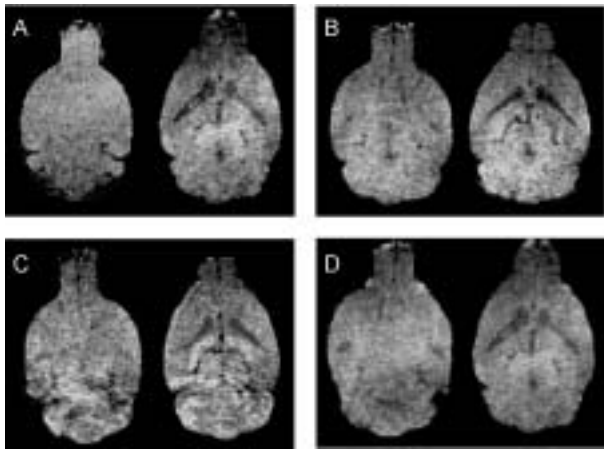

Figure 3. Time course of experimental autoimmune encephalitis (EAE) in the brain from SJL mouse (Jackson Laboratories). Shown are two cross-sections of T1-weighted magnetic resonance microscopy (MRM) images recorded at different time points. **A.** Day 14 (relatively small infiltrates of labeled CD4+ T-cells are seen in the quadrigeminal area). **B.** Day 21 (high signal areas include the parahippocampal areas, brain stem, cerebellum, temporal and frontal lobes). **C.** Day 25 (as the condition resolves, enhancement is less pronounced than in B). **D.** Day 28 (with further resolution of the inflammation, enhancement is even less).

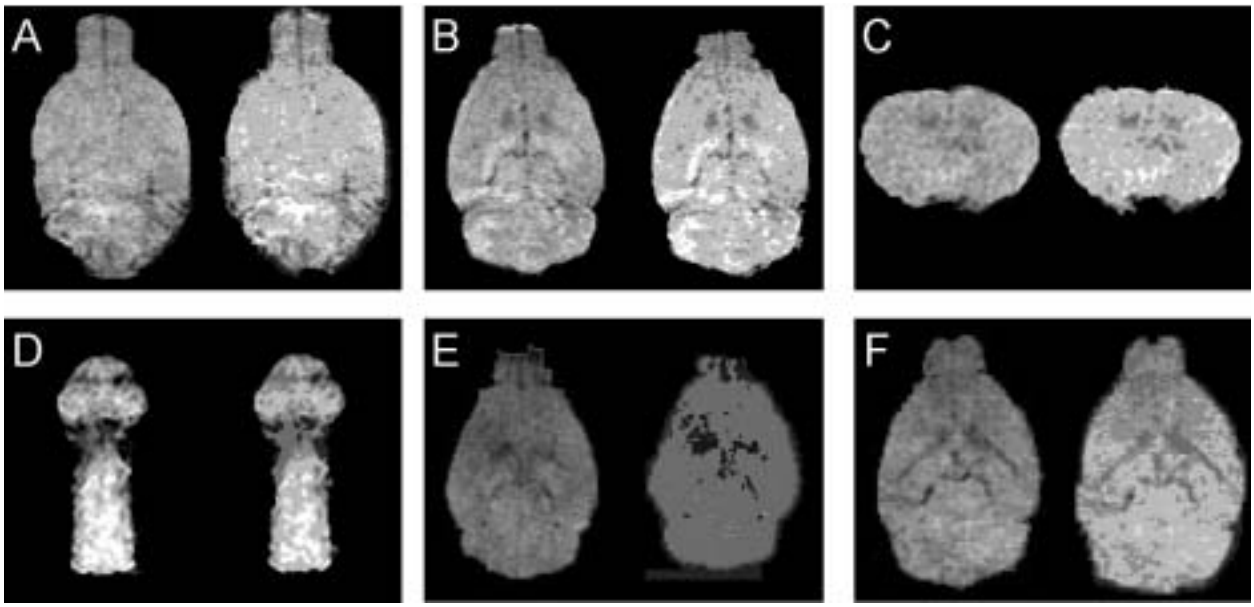

Figure 2. T1-weighted magnetic resonance microscopy (MRM) images of CD4+ T cells in the brain and spinal cord of animals with experimental autoimmune encephalitis (EAE). Each panel shows standard 8-bit image on the left and a 3-bit image on the right. A 3-bit representation obscures morphological details but enhances contrast and improves detection of regions with accumulated ultrasmall superparamagnetic iron oxide particles (USPIOs): A-D images were obtained following the administration of CD4+ T-cell specific contrast material. **A, B**. Axial cuts of the brain including the brain stem, thalamus, hypothalamus, hippocampus, and lateral ventricles. **C.** Coronal cut through the lateral ventricles anterior to the foramen of Monroe. **D.** Coronal view of the brainstem and cervical cord. **E.** Control: healthy brain. **F.** Control: USPIO-labeled human CD19 antibodies in EAE mouse brain. USPIO-labeled anti-CD4 antibodies resulted in enhancement of T1 relaxation, which resulted in the increase of image brightness (A-D). USPIO-labeled anti-CD4 antibodies did not localize in the healthy brain, thus leaving the image contrast unaffected (E). USPIO-labeled human CD19 antibodies only resulted in non-specific background signal enhancement (F).

place and converted them from "invisible into visible" on T1-weighted images. Our hypothesis is that superparamagnetic beads undergo biodegradation that releases iron ions from microbeads core and may put it in direct contact with water in the surrounding environment. This results in changes of proton relaxation times and consequently signal enhancement in T1-weighted images. It is well established that paramagnetic compounds need to be in direct contact with water to exert their effect on proton relaxation time. Since we did not test any superparamagnetic microbeads other than biodegradable, we cannot be certain if the delay of their appearance on T1-weighted images is due to initial shielding from the surrounding water by polysaccharide envelope. Perhaps this can readily be tested by comparison of biodegradable microbeads and those that have a resistant polystyrene envelope. This target-selective imaging method can be considered the in vivo equivalent to immunohistochemistry. Previously defined in vivo lymphocyte-imaging strategies require adoptively transferred cells that are labeled with contrast material ex vivo (14,28-30). To image unaltered lymphocytes in vivo, there have been attempts to target immune cells by injecting Gd-conjugated antibodies (15,16,31-33). These attempts have been technically challenging due to difficulties in appropriately labeling the antibodies. Approximately 100-1,000 Gd atoms need to be attached to a single antibody. This often results in a loss of antigen specificity (17-19). USPIO-based contrast materials are detectable by MRI in nanomolar concentrations making this technology more feasible for imaging specific cell types (33,34). Therefore, we propose to use antibodies labeled with USPIO particles for robust, reproducible antigen-targeted *in vivo* MR imaging. As illustrated above, USPIO-labeled CD4 antibodies allow visualization of CNS infiltrating helper lymphocytes in experimental autoimmune encephalitis. This also allowed us to monitor the dynamics of this process by imaging the animals at multiple time points without sacrificing them. By using this method, one could potentially distinguish between the experimental autoimmune encephalitis susceptibility of various transgenic mouse strains, determine how soon the immune response is initiated, and enable monitoring the infiltration of the studied immune cells of interest.

Native USPIO particles are completely biodegraded in seven days. Because of this property, USPIOs are gaining acceptance in clinical applications (23, 25,35). Superparamagnetic antibodies similar to those used for our technique are currently approved for selecting and enriching human CD34-positive hematopoietic progenitor cells from leukapheresis products (36). These cells have been shown to reconstitute all lineages of immune cells when reinfused into patients that received myeloablative chemotherapy. Since we use superparamagnetic antibodies similar to those approved for human use, it is possible that this technique could be readily developed for human diagnostic use. One of the most challenging imaging problems is to find metastases, infiltrated lymph nodes, or subclinical cancers. Usually, costly and potentially dangerous imaging methods, such as positron emission tomography (PET) or single positron emission computed tomography (SPECT), are used for this purpose, despite low sensitivity and poor resolution. By using USPIO-based targeted contrast materials, the need for such studies could be reduced or eliminated.

In conclusion, we demonstrate the use of USPIO-labeled antibodies originally designed and produced for magnetic cell sorting as an effective contrast agent to selectively visualize immune cells of interest in various CNS inflammations. On the examples of $CD4^+$ T-cells (experimental autoimmune encephalitis), we demonstrated the feasibility of using T1-weighted MR images to follow in a noninvasive way cell's distribution in the CNS. We believe that the same method can easily be applied in human medicine.

Acknowledgments

This work was supported by grants from the National Multiple Sclerosis Society and from the National Institute of Health (No. R01-NS32129 and P01-NS38468).

References

1 Rodriguez M, Miller DJ. Immune promotion of central nervous system remyelination. Prog Brain Res 1994; 103:343-55.

2 Miller DJ, Bright JJ, Sriram S, Rodriguez M. Successful treatment of established relapsing experimental autoimmune encephalomyelitis in mice with a monoclonal natural autoantibody. J Neuroimmunol 1997;75:204-9.

3 Stark DD, Bradley WG, editors. Magnetic resonance imaging. 3rd ed. St. Louis: Mosby; 1999.

4 Callaghan PT. Principles of nuclear magnetic resonance microscopy. Oxford: Clarendon Press; 1991.

5 Ogawa S, Lee TM, Kay AR, Tank DW. Brain magnetic resonance imaging with contrast dependent on blood oxygenation. Proc Natl Acad Sci USA 1990;87:9868-72.

6 Prescott DM, Charles HC, Sostman HD, Dodge RK, Thrall DE, Page RL, et al. Therapy monitoring in human and canine soft tissue sarcomas using magnetic resonance imaging and spectroscopy. Int J Radiat Oncol Biol Phys 1994;28:415-23.

7 Walpoth BH, Galdikas J, Tschopp A, Vorburger T, Lazeyras F, Schaffner T, et al. Differentiation of cardiac ischemia and rejection by nuclear magnetic spectroscopy. Thorac Cardiovasc Surg 1991;39 Suppl 3:217-20.

8 Caravan P, Ellison JJ, McMurry TJ, Lauffer RB. Gadolinium(III) chelates as MRI contrast agents: structure, dynamics, and applications. Chem Rev 1999;99:2293-352.

9 Merbach AE, Tâoth Â. The chemistry of contrast agents in medical magnetic resonance imaging. Chichester (NY): Wiley; 2001.

10 Louie AY, Huber MM, Ahrens ET, Rothbacher U, Moats R, Jacobs RE, et al. In vivo visualization of gene expression using magnetic resonance imaging. Nat Biotechnol 2000;18:321-5.

11 Poduslo JF, Wengenack TM, Curran GL, Wisniewski T, Sigurdsson EM, Macura SI, et al. Molecular targeting of Alzheimer's amyloid plaques for contrast-enhanced magnetic resonance imaging. Neurobiol Dis 2002;11: 315-29.

12 Anderson-Berg WT, Strand M, Lempert TE, Rosenbaum AE, Joseph PM. Nuclear magnetic resonance and gamma camera tumor imaging using gadolinium-labeled monoclonal antibodies. J Nucl Med 1986;27: 829-33.

13 Cerdan S, Lotscher HR, Kunnecke B, Seelig J. Monoclonal antibody-coated magnetite particles as contrast agents in magnetic resonance imaging of tumors. Magn Reson Med 1989;12:151-63.

14 Rosenthal SG, Willich HC, Ebert W, Conrad J. The demonstration of human tumors on nude mice using gadolinium-labeled monoclonal antibodies for magnetic resonance imaging. Invest Radiol 1993;28:789-93.

15 Yeh TC, Zhang W, Ildstad ST, Ho C. Intracellular labeling of T-cells with superparamagnetic contrast agents. Magn Reson Med 1993;30:617-25.

16 Yeh TC, Zhang W, Ildstad ST, Ho C. In vivo dynamic MRI tracking of rat T-cells labeled with superparamagnetic iron-oxide particles. Magn Reson Med 1995; 33:200-8.

17 Weissleder R, Cheng HC, Bogdanova A, Bogdanov A Jr. Magnetically labeled cells can be detected by MR imaging. J Magn Reson Imaging 1997;7:258-63.

18 Franklin RJ, Blaschuk KL, Bearchell MC, Prestoz LL, Setzu A, Brindle KM, et al. Magnetic resonance imaging of transplanted oligodendrocyte precursors in the rat brain. Neuroreport 1999;10:3961-5.

19 Dousset V, Delalande C, Ballarino L, Quesson B, Seilhan D, Coussemacq M, et al. In vivo macrophage activity imaging in the central nervous system detected by magnetic resonance. Magn Reson Med 1999;41: 329-33.

20 Häfeli U, Schütt W, Teller J, Zborowski M, editors. Scientific and clinical applications of magnetic carriers. New York: PLENUM Press; 1997.

21 Su XM, Sriram S. Treatment of chronic relapsing experimental allergic encephalomyelitis with the intravenous administration of splenocytes coupled to encephalitogenic peptide 91-103 of myelin basic protein. J Neuroimmunol 1991;34:181-90.

22 Huber JD, Egleton RD, Davis TP. Molecular physiology and pathophysiology of tight junctions in the blood-brain barrier. Trends Neurosci 2001;24:719-25.

23 Owens T, Wekerle H, Antel J. Genetic models for CNS inflammation. Nat Med 2001;7:161-6.

24 Nau R, Bruck W. Neuronal injury in bacterial meningitis: mechanisms and implications for therapy. Trends Neurosci 2002;25:38-45.

25 Meli DN, Christen S, Leib SL, Tauber MG. Current concepts in the pathogenesis of meningitis caused by Streptococcus pneumoniae. Curr Opin Infect Dis 2002;15: 253-7.

26 Stohlman SA, Hinton DR. Viral induced demyelination. Brain Pathol 2001;11:92-106.

27 Pirko I, Johnson A, Ciric B, Gamez J, Macura S, Pease L, et al. In vivo magnetic resonance imaging of immune cells in the central nervous system with superparamagnetic antibodies. FASEB J. Forthcoming 2003.

28 Hudgins PA, Anzai Y, Morris MR, Lucas MA. Feruмoxtran-10, a superparamagnetic iron oxide as a magnetic resonance enhancement agent for imaging lymph nodes: a phase 2 dose study. AJNR Am J Neuroradiol 2002;23:649-56.

29 Dousset V, Gomez C, Petry KG, Delalande C, Caille JM. Dose and scanning delay using USPIO for central nervous system macrophage imaging. MAGMA 1999; 8:185-9.

30 Lauffer RB. Paramagnetic metal complexes as water proton relaxation agents for NMR imaging: theory and design. Chem Rev 1987;87:901-27.

31 Akiyama H, Arai T, Kondo H, Tanno E, Haga C, Ikeda K. Cell mediators of inflammation in the Alzheimer disease brain. Alzheimer Dis Assoc Disord 2000;14 Suppl 1:S47-53.

32 Costa GL, Sandora MR, Nakajima A, Nguyen EV, Taylor-Edwards C, Slavin AJ, et al. Adoptive immunotherapy of experimental autoimmune encephalomyelitis via T cell delivery of the IL-12 p40 subunit. J Immunol 2001;167:2379-87.

33 Sweeney TJ, Mailander V, Tucker AA, Olomu AB, Zhang W, Cao Y, et al. Visualizing the kinetics of tumor-cell clearance in living animals. Proc Natl Acad Sci U S A 1999;96:12044-9.

Received: May 13, 2003
Accepted: June 25, 2003

Correspondence to:
Slobodan Macura
Department of Biochemistry
Mayo Clinic
200 1st Street SW
Rochester, MN 55905, USA
macura@mayo.edu